A CONCRETE RHEOMETER: FEATURES AND INDUSTRIAL APPLICATIONS

Faber Fabbris[1*], Walter De Carvalho[2], Didier Lootens[3]

[1] Technical Service BU Concrete, Sika France S.A.S, Le Bourget, FRANCE.
[2] Concrete Laboratory, Technology Center, Sika France S.A.S., Gournay, FRANCE.
[3] Material Physics, Sika Technology AG, Zürich, SWITZERLAND.

*: corresponding author. fabbris.faber@fr.sika.com

ABSTRACT

Concrete flow properties are usually measured with the slump test, V-funnel or L-box, which give robust but limited information on the rheological properties of the complex suspension. In order to complete the analysis obtained with the classical techniques, a new speed controlled rheometer, especially conceived for concrete and cement based products, has been developed by upgrading an existing commercial device. By a 'Couette like' approach, concretes ranging from S4 consistency up to SCC have been quantitatively characterized with a measurement range spread over 4 logarithmic decades. Extended rheological characterizations of concrete are made in the quasi-steady and transient regimes, where the thixotropic behavior can be observed. A series of applications are presented to demonstrate the possibility to quantify the impact of the admixture type on the flow of concretes and cement based system. Such an approach solves practical industrial problems, which could not be fixed with the classical technological tests.

Keywords: concrete; rheology; rheometer; thixotropy

INTRODUCTION

The interest of a quantitative, precise featuring of concrete flow properties has widespread considerably during the last decades. This was essentially due to the growing impact of polycarboxylic-polyacrylic superplasticizers, as well as the development of precasting in building techniques. The development of technological tests [i] as well as the introduction of new standards [2] demonstrate the growing interest of quantitative rheological

measurements for cementitious materials. The main virtue of technological tests is obviously their simplicity and ease of execution, letting on yard as well as lab testing. On the other hand, they all deserve the same limit, as they all provide a metric parameter as a result, but do not let to access intrinsic, intensive physical quantities [3]. Moreover, the results of each technological test generally depend on several rheological properties simultaneously such as yield stress, viscosity or thixotropic phenomena, making difficult the establishment of injective relationships between two classes of data. The need for a more precise characterization of concrete behaviour, either for theoretical and practical reasons, has promoted the development of specific devices, namely rheometers, which have been reviewed and compared in several technical reports [4, 5]. All these tools greatly contributed to the progress of concrete rheology; unfortunately they are limited by the extent of measurement, rarely overpassing one logarithmic decade for velocity gradient values [5]. The development of a speed controlled concrete rheometer, shortly presented in [6], let us to enlarge the accessible values of velocity gradients and consequently give a deeper analysis of concrete flow behaviour.

APPLICATION OF 'COUETTE-LIKE' APPROACH AND TECHNICAL FEATURES OF THE RHEOMETER

In the case of multiscale, multiphase systems such as cement based materials, cylindrical surfaces don't fit the adherence condition between the 'fluid' and the walls of the vessels, and we can not, consequently, fix the boundary conditions for their motion [7,8]; moreover, phase separation phenomena may occur, thus vanishing the purpose of an homogeneous gradient between the two Couette surfaces [9]. 'Unconventional' mobiles such as 'vanes', helical shaped mobiles or other 'impeller-like' mobile, may overpass this problem but oblige to make some theoretical assumption and experimental preliminary measurements. The device presented here has been developed on the basis of a commercial, RheoCAD 500 by CAD Instrument, France. The features of this machine are shortly summarized in Table 1.

Table 1. Mechanical features of RhéoCAD 500

Physical quantity	Rotational speed	Torque on crankshaft
Minimum value	10^{-3} rpm = $1{,}047 \cdot 10^{-4}$ rad/s	10^{-3} N·m
Maximum value	250 rpm = $2{,}6175 \cdot 10^{1}$ rad/s	10 N·m
Resolution	10^{-3} rpm = $1{,}047 \cdot 10^{-4}$ rad/s	10^{-3} N·m

For a given couple of agitator (mobile) and confinement device (vessel), the possibility of using such a controlled crankshaft as a rotational rheometer relies on the definition of an

equivalent cylindrically symmetric shear stress field and an equivalent homogeneous velocity gradient (both of radius R_i). This can be done with the well-know 'Couette-like' approach [10,11,12]. The main assumption of this method is that the behaviour of the system which undergoes the flow can be described analytically by a power law dependency. The method essentially aims to establish the two constants $K_{\dot{\gamma}}$ and K_τ defined respectively as the ratio of the shear rate $\dot{\gamma}$ over the rotational speed N and as the shear stress τ over the torque Γ on rheometer crankshaft. The determination of the equivalent internal radius, R_i has been done for many mobile/vessel configurations, by using a series of Newtonian fluids, on the basis of the equation (1); (L is the height of immersed mobile and R_e the vessel radius). For a Newtonian fluid N/Γ being proportional to the inverse of viscosity, the value of R_i is a constant. For a power law fluid, the shear rate is given by equation (2).

$$R_i = R_e/(1 + 8\pi^2 L\, R_e^2 \eta\, (N/\Gamma))^{\frac{1}{2}} \tag{1}$$

$$\dot{\gamma}(r, n, N) = \frac{4\pi N}{n} \frac{(R_i/r)^{2/n}}{1 - (R_i/R_e)^{2/n}} \tag{2}$$

n being the fluid index. Indeed, the variation of $\dot{\gamma}$ along the radius would not let to fix $K_{\dot{\gamma}}$. Nevertheless, it can be shown [11] that for a given radius value, indicated by r^*, the variation of $\dot{\gamma}$ as a function of n is a minimum. This value may be taken as the reference radius for estimating the velocity gradient and the shear stress constants. The relevant rheometric parameters are shown for the different mobiles/vessels on Table 2.

$$K_{\dot{\gamma}} = \frac{\dot{\gamma}(r^*, N)}{N} = \frac{4\pi}{n} \frac{(R_i/r^*)^2}{1 - (R_i/R_e)^2} \tag{3}$$

$$K_\tau = \frac{\tau}{\Gamma} = \frac{1}{2\pi r^{*2} L} \tag{4}$$

We stress that the validity of (2) and (3) is in principle limited to the cases for which the velocity gradient can be considered as –almost approximately- homogeneous. For yield stress fluids, as we can roughly model cement based systems [13], the appearance of unsheared regions for low gradient values [14,15,16] implies that these relations stand only above the 'yield stress' limit, i.e. for fully developed, power law described, velocity fields (see further).

Table 2. Geometric features, rheometric constants, measurement limits of some mobile/vessel coupling. The one used for concrete measurements (see next paragraphs) is shaded in light grey.

Mobile/vessel	R_i	R_e	r^*	$K_{\dot{\gamma}}$	K_τ	$\dot{\gamma}_{min}$-$\dot{\gamma}_{max}$	τ_{min}-τ_{max}
Units	m	m	m	$(rpm{\cdot}s)^{-1}$	m^{-3}	s^{-1}	Pa
CMB C GV 12	0,055	0,118	0,067	1,75	140,5	$1{,}75{\cdot}10^{-3}$ - 440	0,14 - 1400
CMB C DSH12	0,047	0,118	0,059	1,60	179,8	$1{,}6{\cdot}10^{-3}$ - 400	0,12 - 1200
CMB C DSH16	0,064	0,118	0,077	2,01	106,7	$2{\cdot}10^{-3}$ - 500	0,11 - 1100
CMB C DSH-19	0,071	0,118	0,085	2,37	113,9	$2{,}4{\cdot}10^{-3}$ - 590	0,11- 1140

The superposition of shear rate as a function of the shear stress curves for different Newtonian fluids and the various measurement configurations (mainly helically shaped, and adapted to different materials) is represented in the right graphic of Figure 2. All the measurements are almost independent on the measuring equipment in the shear rate range of $2{,}5 \cdot 10^{-2}$ s^{-1} to $2{,}5 \cdot 10^{2}$ s^{-1}, and with a standard deviation lower than 7 %. At lower velocities, edge effects appear, with an over/underestimation of the torque, resulting essentially from cinematic effects. A correction of these effects by considering $K_{\dot{\gamma}}$ and K_{τ} as functions of rotational speed is possible, but not presented in this work.

Figure 2. Torque as a function of the rotation speed for different Newtonian fluids (left), superposed rheograms of the same Newtonian fluid, obtained with all the mobile/vessel coupling (right).

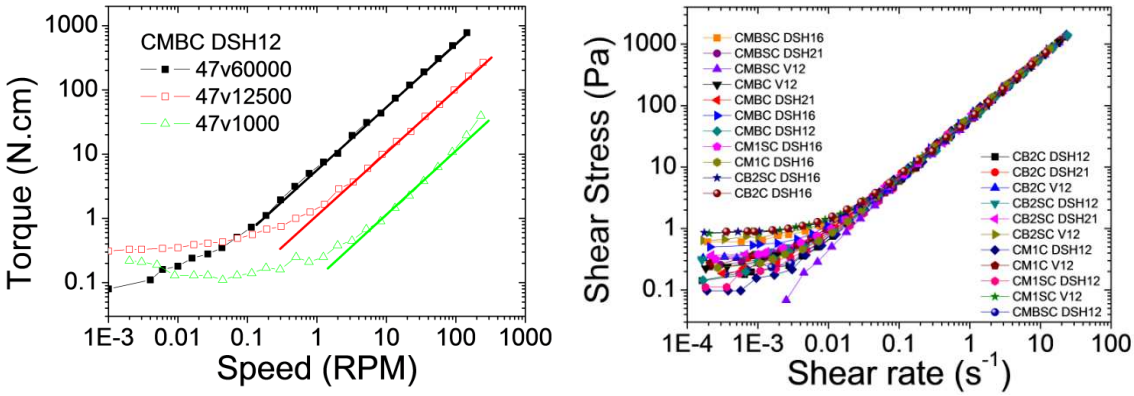

The choice of a mobile/vessel coupling depends on system's features. While for higher r^* and R_e values and for smaller extent of gap (R_e - r^*), we get smaller velocity gradient dependencies on r, the maximum size of aggregates (D_{max}) may impose to choice wider gap values. For lower viscosities (SCC, screeds) the limiting parameter is rotational speed (centrifugation effects); for high viscosity or high yield stress materials, the limiting parameter is the maximum torque. In this case, the choice of a mobile/vessel couple with lower radii let to increase the maximum shear stress for a given torque. The almost total independency of results on the choice of tools let to compare measurements even when performed with different devices. For measurements on concretes, (consistency from S4 to SCC), we used a vessel coupled with a double helical mobile (see table 2 for features).

EFFECT OF SUPERPLASTICIZERS ON THE SAME CONCRETE FORMULATION

The standard measurement protocol includes two series of downward, upward velocity imposed steps, logarithmically spaced. The upper limit is set by the instrument (maximum

toque or speed). The number of steps for each logarithmic decade is fixed to 5 with a maximum duration of 15s. Conversely, the evolution of the shear stress as a function of the shear strain is obtained by associating the equilibrium values of shear stress to the corresponding velocity gradient (Fig. 3). The protocol enables to measure the evolution of the shear stress over at least three decades but also to access the typical thixotropic behaviour of suspended particle systems: a hysteresis between the down and the up curve, and the presence of a yield stress region. For higher values of the velocity gradient, we access the linear region of shear stress/velocity gradient dependency, (asymptotic approach of the curve to the n-slope in logarithmic diagram).

Figure 3. Shear stress as a function of the velocity gradient for a SCC.
L: shear stress, shear rate vs. time. R: shear stress vs. shear rate. Measure tool: CMB C DSH12 in Table 2

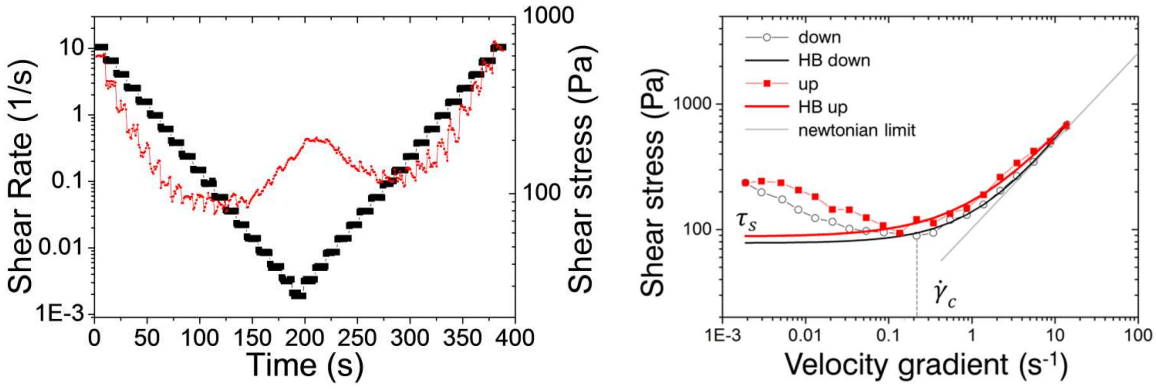

The minimum value for shear stress, corresponding to the critical gradient $\dot{\gamma}_c$ (and indicated by τ_s), stands as the point for which the tendency of the system to rebuilt at rest overcomes the applied shear field: below this value, the shear stress increase even when lowering the rotational speed. This is essential for understanding the technological features of concretes, as it leads their behaviour in the transition between flow and rest conditions (thixotropy). The application of a Herschel-Bulkley model (Eq. 5) on the "down" curve[1] is used to fit data, by assuming $\tau_0 \approx \tau_s = \tau(\dot{\gamma}_c)$, and considering the values for which $\dot{\gamma} > \dot{\gamma}_c$.

$$\tau = \tau_s + \eta_{pl}\dot{\gamma}^n \quad (5)$$

This implies to consider the critical gradient value as the lowest for which the velocity field is completely developed (and hence the eqs. 2 and 3 may be applied). Below this value, the presence of unsheared regions does not let to consider the velocity gradient modulus proportional to the rotational velocity of the mobile [17, 18]. The use of this simple

[1] The 'down' curve is often more representative for many fresh state processes concrete undergoes (poured in casts after mixing in batch plants or mixer truck), as well in their flow history during many technological tests (Abrams cone, L-box, J ring).

model let to associate four parameters for each curve: $\dot{\gamma}_c$ (s-1), τ_s (Pa), η_{pl} (Pa·s^n), n (dimensionless). Notwithstanding its necessarily incomplete and merely conventional character [19,20], this parameterization may be used just in order to obtain a synthetic and comparative analysis of measurement results. As an application of this measurement technique, we compare the effect of different kind of superplasticizers on the same concrete SCC formulation, prepared with a W/C of 0,6 and a paste volume of 0,375. The maximum aggregates diameter is 12,5mm. For simplicity, we shall consider only the 'down' curve. In addition to the rheological curve, the results of Abrams cone test (slump flow) and V-funnel test (emptying times) are indicated. The effects of 4 different superplasticizers are shown on figure 4.

Figure 4. Rheograms of SCC admixed with different dosages of Polymer A, B, C and D.

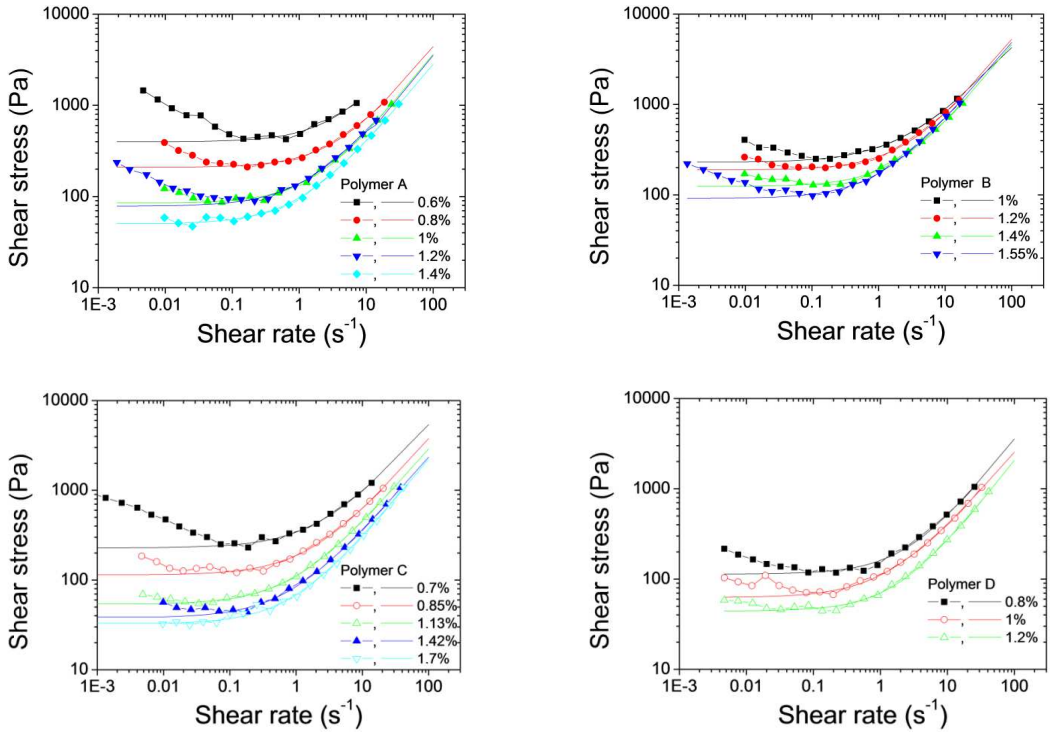

We can see the wide modifications induced by superplasticizer A. More precisely, we have a reduction of the critical velocity gradient $\dot{\gamma}_c$, a lowering of corresponding yield stress τ_s and a reduction of η_{pl}. A résumé of the values of rheological parameters is presented on Table 3, including the value of apparent viscosity at 20s^{-1} ($\eta_{20/s}$). The higher dosage tested, 1,4% of cement and filler mass, resulted in concrete phase segregation (superplasticizer overdosage). This fact is well witnessed by the evolution of τ_s, converging towards a limit value (roughly 75Pa) up to 1,2% dosage; further superplasticizer addition determines a drop of τ_s. Analogous considerations may be done for the evolution of critical gradient $\dot{\gamma}_c$. The reduction of plastic viscosity as well as yield stress means that

this admixture acts both on the 'rest' organization of the matter as well as the 'flow' one.

Table 3. Values of rheological parameters for different dosages of polymer A, B, C and D.

	Dosage	τ_s	$\dot{\gamma}_c$	η_{pl}	$\eta_{20/s}$	n	E_{tl}	t_{vf}
	%	Pa	s^{-1}	$Pa{\cdot}s^n$	Pa·s	-	mm	s
Superplasticizer A	0,60	399,0	0,63	110,4	55,0	0,93	420	6,0
	0,80	209,0	0,17	60,8	58,3	0,92	545	5,6
	1,00	84,7	0,10	51,0	44,6	0,93	640	4,9
	1,20	78,1	0,10	60,4	45,9	0,87	690	4,6
	1,40	50,0	0,06	46,8	35,7	0,88	700	3,7
Superplasticizer B	1,00	228,4	0,18	109,2	68,6	0,78	465	5,2
	1,20	188,9	0,16	75,8	67,9	0,91	525	6,1
	1,40	123,8	0,13	63,5	56,8	0,92	605	6,1
	1,55	91,1	0,10	81,6	62,1	0,88	640	6,3
Superplasticizer C	0,70	228,5	0,19	112,1	79,2	0,82	470	5,3
	0,85	113,7	1,12	73,1	52,3	0,85	605	5,1
	1,13	53,6	0,04	57,2	28,9	0,84	690	3,9
	1,42	37,9	0,18	46,3	23,4	0,85	740	3,6
	1,70	32,5	0,02	36,1	22,2	0,89	775	3,0
Superplasticizer D	0,60	531,7	0,59	79,5	134,2	1,00	365	7,6
	0,80	113,7	0,21	46,8	44,1	0,93	605	4,1
	1,00	62,4	0,20	47,9	34,3	0,86	690	3,1
	1,20	44,2	0,14	25,8	24,3	0,95	755	3,1

A comparison with Admixture B shows the different tendencies of its way of action (upper right graphic of Fig. 4). We have here a fundamentally different action than the superplasticizer A: the critical velocity gradient $\dot{\gamma}_c$ stills essentially unchanged with a lowering of yield stress τ_s but the plastic viscosity almost constant. A synthetic presentation of the rheological analysis and technological tests results is shown on Table 3. A comparison with admixture A let to observe that Admixture B has no or low impact on the organization of matter in flow conditions (same plastic viscosity), and that his action is essentially limited to reduce the yield stress. This can be indirectly appreciated by V-funnel values. In the case of polymer C, we can appreciate both a reduction of critical gradient and plastic viscosity, up to a minimum value corresponding to concrete instability (no rebuilt under the critical gradient). Finally, polymer D keeps an unchanged value of the critical gradient overall the tested dosages, acting both on plastic viscosity and yield stress.

CONCLUSIONS

The rheological analysis, performed with RheoCAD equipped with different measuring tools, let us to access a detailed characterization of concrete flow behaviour. The

extent of the measurement allows a wide, detailed rheometric survey. The comparison of different superplasticizer is an example of different type of rheological impact of these substances, linked to their different way of action. This is an useful tool to access and solve industrial problem of concrete processing and use, in an unified and quick way, whereas the technological test reflect each some different aspect of flow properties, and often a superposition of their effects.

LIST OF REFERENCES

1. The European Guidelines for Self-Compacting Concrete. Specification, Production and Use, A BIBM, CEMBUREAU, ERMCO, EFCA, EFNARC Publication, 2005, pp. 43-59.

2. Norme NF 206-9, règles complémentaires pour le béton auto-plaçant, 2010.

3. N. Roussel, P. Coussot, "Fifty-cent rheometer" for yield stress measurements: From slump to spreading flow. Journal of rheology, Vol 49, 2005, pp. 705-718.

4 . Ferraris, C. F., Brower, L.E. (eds.) Comparison of Concrete Rheometers: International Tests at LCPC (Nantes, France) in October 2000. NIST Internal Report 6819, Springfield, 2001.

5. Ferraris, C. F., Brower, L.E. (eds.) Comparison of concrete rheometers: International tests at MB Cleveland OH, USA in May, 2003. NIST Internal Report 7154, Springfield, 2004.

6. Fabbris, F., de Carvalho, W., Le comportement rhéologique de la pâte de ciment et sa comparaison avec celui du béton : techniques de mesures et analogies d'échelles. Actes du 44ème colloque du Groupe Français de Rhéologie, Strasbourg, 2009, pp. 225-228.

7. Kaylon, D.M., Apparent Slip and viscoplasticity of concentrated suspensions, Journal of Rheology, Vol. 49, 2005, pp. 621-640.

8. Reiner, M., Deformation, Strain and Flow, London, 1960.

9. Leighton, D., Acrivos, A., The shear-induced migration of particles in concentrated suspensions, Journal of Fluid Mechanics, Vol. 275, 1987, pp. 155–199.

10. Bousmina, M., Aït-Kadi, A., Determination of shear rate and viscosity from batch mixer data, Journal of Rheology, Vol. 43, 1999, pp. 415-433.

11. Bousmina, M., Aït-Kadi, A., Quantitative Analysis of Mixer type Rheometers using the Couette Analogy, The Canadian journal of chemical engineering, Vol. 80, 2002.

12. Brito de la Fuente et al., A New Investigation of Metzner-Otto Concept for Anchor mixing Impellers, The Canadian journal of chemical engineering, volume 74, 1996, pp. 222-228.

13. De Larrard, F., Ferraris, C.F., Sedran, T., Fresh concrete: a Herschel-Bulkley material, Materials and Structures/Matériaux et Constructions, Vol. 31, 1998, pp. 494-498.

14. Jarnya, S., Roussel, N., Rodts, S., Bertrand, F., Le Roy, R., Coussot, P. Rheological behavior of cement pastes from MRI velocimetry, Cement and Concrete Research, Vol. 35, 2005, pp. 1873-1881.

15. Wiederseiner, S., Ancey, C., Andreini, N., Rentschler, M., Rhéophysique des suspension granulaires très concentrées par vélocimétrie par images de particules fluorescentes, Congrès Francophone de Techniques Laser, Poitiers, 2008.

16 Takeda, Y., Velocity profile measurement by ultrasonic doppler method, Experimental Thermal and Fluid Science, Vol.10, 1995, pp.444–453.

17. Coussot, P., Huynh, H.,T., Nguyen, Q.D., Bonn, D., Viscosity bifurcation in thixotropic, yielding fluids, Journal of Rheology, Vol.46, 2002, pp. 573-589.

18. Chatzimina M., Georgiou G., Alexandrou A., Wall shear rates in circular Couette flow of a Herschel-Bulkley fluid, Applied Rheology, Vo. 19, 2009, pp. 34288-34296.

20. Barnes, H.A., The yield stress-a review or ' πάντα ῥεῖ '- everything flows?, Journal of non newtonian fluid Mechanics, vol. 81, 1999, p.133-178.

21. Barnes, H.A., The yield stress myth?, Rheologica Acta, Vol.24, 1985, pp.323-326.